COMPUTER-AIDED MODELING OF A RECTIFIED DC LOAD-PERMANENT MAGNET GENERATOR SYSTEM WITH MULTIPLE DAMPER WINDINGS IN THE NATURAL abc FRAME OF REFERENCE

A.A. Arkadan, Member
Marquette University
Milwaukee, WI.

T.M. Hijazi, Member
Clarkson University
Potsdam, N.Y.

N.A. Demerdash, Senior Member

Abstract - A computer-aided modeling method, by which one can analyze and predict the dynamic performance of electronically rectified load-permanent magnet generator systems is presented. These generators include multiple damping circuits. Continuous electronic switching in such systems results in a continuous change in the machine system network topologies. Hence, network modeling of such systems was done here on an instantaneous basis. In this work, the natural abc frame of reference was used throughout. This is an advantage in that effects of magnetic nonlinearities, space harmonics in the mmfs, and space harmonics in the flux density waveforms as well as winding flux linkages on all machine parameters were readily taken into account. This method was applied to a two-pole, 75 kVA, 208 V, 24000 r/min permanent magnet generator, to study the generator-load system performance. Furthermore, the use of the model in studying rotor damping design options and effects of electronic component failure in the associated rectifier bridge on the generator-rectifier load system performance, is given.

KEYWORDS:
Permanent Magnet Generators
Rectified DC Load
Damper Windings

INTRODUCTION

Modeling and analysis of the performance of rotating electric machinery interfaced with electronic power conditioning devices such as inverters and rectifier bridges can be found throughout the literature. A sample of such work is references [1] through [6]. In such systems, the continuous switching taking place in the electronic power conditioning components means that the corresponding network topologies of these systems are undergoing continuous and cyclical changes. This means that steady state operation is in reality a "dynamic steady state" as explained in references [4-6]. In this paper, a computer-aided method based on the utilization of the natural abc frame of reference is presented for the analysis and prediction of the steady state dynamic performance of electronically rectified load-permanent magnet generator systems with multiple damping circuits. Furthermore, the method and the resulting model were used to study the effects of electronic component failure in the associated rectifier bridge on generator-rectifier load system performance.

In the present approach applied to a 75 kVA, 208 V, 24000 r/min permanent magnet (PM) generator [7,10], Figure (1), which utilizes the natural abc frame of reference, both saliency and damping circuits' effects were included. In addition, the inherent harmonics in the flux linkages, inductances, as well as those in the induced emfs were accounted for. The nonlinear self and mutual inductances of the various machine windings and the induced emfs were obtained using finite element magnetic field solutions, as was demonstrated in an earlier paper [7].These inductances and emfs, see the Appendix, are the key parameters in the state models which were used in this work. Another important advantage of using this approach, is that it makes it easier to incorporate such abc machine models into an overall modeling effort of the system network including rectifier loads, such as the one shown in Figure (2), which are inherently in the abc frame of reference. The state equations which govern the dynamic performance of this system, Figure (2), were automatically generated using generalized concepts of network graph theory and the hybrid matrix formulation of nonlinear networks [9]. The main components of this modeling approach (finite element, hybrid matrix formulation) were verified experimentally in an earlier work by these authors [11-13].

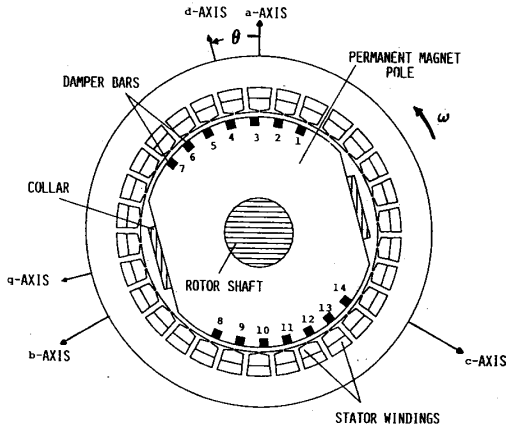

Figure (1): Permanent Magnet Generator Cross-Section

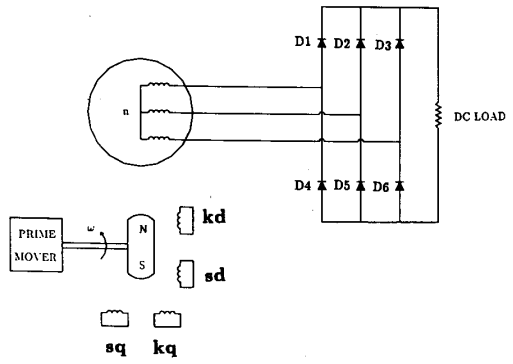

Figure (2): Permanent Magnet Generator-Rectifier Load System Schematic Diagram

In this paper, the results of simulation of the 75 kVA generator-rectifier load system performance, as well as assessment of the impact of several rotor damping design options on the system performance, are studied. In addition, the impact of incorporation of the damping effects on the overall generator-load system power is studied. Finally, the use of the model in studying effects of electronic component failure in the associated rectifier bridge on the generator-rectifier load system performance, is given.

89 WM 225-4 EC A paper recommended and approved by the IEEE Rotating Machinery Committee of the IEEE Power Engineering Society for presentation at the IEEE/PES 1989 Winter Meeting, New York, New York, January 29 - February 3, 1989. Manuscript submitted August 2, 1988; made available for printing November 29, 1988.

PERMANENT MAGNET GENERATOR-RECTIFIER LOAD SYSTEM DESCRIPTION

In the generator-rectifier load system of Figure (2), the machine is a two pole, 75 kVA, 208 V, 24000 r/min permanent magnet (PM) generator which consists of a three phase (stator) armature winding connected to a three phase full wave rectifier bridge feeding a dc load. The two pole permanent magnet rotating structure, Figure (1), represents the field. A metallic damping ring (collar), which is fitted around the rotor structure, acts as a shorted winding. The ring aids the damping effects caused by the 14 damper bars (damper cage) which are embedded in the faces of the two poles of the rotor's permanent magnets. In Figure (2), as well as in the state models representing the machine, the damper bar cage was replaced by two equivalent windings, kd and kq. Here, kd and kq represent the damping effects along the direct and quadrature axes of the machine, and are both shorted coils. In a similar fashion, the metallic collar was replaced by two equivalent damping windings sd and sq, which represent damping effects along the direct and quadrature axes, respectively. Again, both are shorted coils.

PERMANENT MAGNET GENERATOR MODELING DESCRIPTION

In this section, a description of the method used for modeling the permanent magnet (PM) generator, is given. However, in order to study the impact of addition of a damping metallic ring (collar), mounted around the rotor, on the dynamic performance of the PM generator-rectifier load system, two models were used for the generator. In the first model, in order to study the impact of the simultaneous presence of a damper bar cage and a rotor mounted metallic damping ring (collar) on the dynamic performance of the PM generator-rectifier load system, a seventh order lumped parameter state model must be used. This state model was derived in an earlier paper,[7], and is restated here in equation (1) for purposes of continuity.

$$
\begin{bmatrix} v_a \\ v_b \\ v_c \\ v_{kd} \\ v_{kq} \\ v_{sd} \\ v_{sq} \end{bmatrix} = \begin{bmatrix} r_a & 0 & 0 & 0 & 0 & 0 & 0 \\ 0 & r_b & 0 & 0 & 0 & 0 & 0 \\ 0 & 0 & r_c & 0 & 0 & 0 & 0 \\ 0 & 0 & 0 & r_{kd} & 0 & 0 & 0 \\ 0 & 0 & 0 & 0 & r_{kq} & 0 & 0 \\ 0 & 0 & 0 & 0 & 0 & r_{sd} & 0 \\ 0 & 0 & 0 & 0 & 0 & 0 & r_{sq} \end{bmatrix} \begin{bmatrix} i_a \\ i_b \\ i_c \\ i_{kd} \\ i_{kq} \\ i_{sd} \\ i_{sq} \end{bmatrix}
$$

$$
+ \begin{bmatrix} L_{aa} & L_{ab} & L_{ac} & L_{akd} & L_{akq} & L_{asd} & L_{asq} \\ L_{ba} & L_{bb} & L_{bc} & L_{bkd} & L_{bkq} & L_{bsd} & L_{bsq} \\ L_{ca} & L_{cb} & L_{cc} & L_{ckd} & L_{ckq} & L_{csd} & L_{csq} \\ L_{kda} & L_{kdb} & L_{kdc} & L_{kdkd} & L_{kdkq} & L_{kdsd} & L_{kdsq} \\ L_{kqa} & L_{kqb} & L_{kqc} & L_{kqkd} & L_{kqkq} & L_{kqsd} & L_{kqsq} \\ L_{sda} & L_{sdb} & L_{sdc} & L_{sdkd} & L_{sdkq} & L_{sdsd} & L_{sdsq} \\ L_{sqa} & L_{sqb} & L_{sqc} & L_{sqkd} & L_{sqkq} & L_{sqsd} & L_{sqsq} \end{bmatrix} \cdot \frac{d}{dt} \begin{bmatrix} i_a \\ i_b \\ i_c \\ i_{kd} \\ i_{kq} \\ i_{sd} \\ i_{sq} \end{bmatrix}
$$

$$
+ \omega \left\{ \frac{d}{d\theta} \begin{bmatrix} L_{aa} & L_{ab} & L_{ac} & L_{akd} & L_{akq} & L_{asd} & L_{asq} \\ L_{ba} & L_{bb} & L_{bc} & L_{bkd} & L_{bkq} & L_{bsd} & L_{bsq} \\ L_{ca} & L_{cb} & L_{cc} & L_{ckd} & L_{ckq} & L_{csd} & L_{csq} \\ L_{kda} & L_{kdb} & L_{kdc} & L_{kdkd} & L_{kdkq} & L_{kdsd} & L_{kdsq} \\ L_{kqa} & L_{kqb} & L_{kqc} & L_{kqkd} & L_{kqkq} & L_{kqsd} & L_{kqsq} \\ L_{sda} & L_{sdb} & L_{sdc} & L_{sdkd} & L_{sdkq} & L_{sdsd} & L_{sdsq} \\ L_{sqa} & L_{sqb} & L_{sqc} & L_{sqkd} & L_{sqkq} & L_{sqsd} & L_{sqsq} \end{bmatrix} \right\} \cdot \begin{bmatrix} i_a \\ i_b \\ i_c \\ i_{kd} \\ i_{kq} \\ i_{sd} \\ i_{sq} \end{bmatrix}
$$

$$
+ \begin{bmatrix} e_a \\ e_b \\ e_c \\ 0 \\ 0 \\ 0 \\ 0 \end{bmatrix} \tag{1}
$$

where θ is the rotor position angle in electrical radians, measured from a fixed reference, and ω is the angular speed in electrical rad/s. The first term on the right hand side of equation (1) represents the ohmic voltage drop in the seven windings of the machine, that is a, b, c, kd, kq, sd, and sq. Meanwhile, the second term represents the transformer voltage component. Finally, the last two terms represent the rotational voltage components in the three armature phase windings and the four equivalent damper windings.

This set of differential equations, equation (1), can be represented by an equivalent network model as shown in Figure (3), in which the following types of circuit elements are present: resistors, self and mutual inductances, independent voltage sources, and current controlled voltage sources. The resistors, self and mutual inductances, and independent voltage sources are self explanatory. Here, the current controlled voltage sources v_{ar}, v_{br}, v_{cr}, v_{kdr}, v_{kqr}, v_{sdr}, and v_{sqr}, represent the rotational voltage coupling (the loading effect) in a coil due to its own current as well as the currents in the six remaining equivalent machine coils. Based on the third term of equation (1), these current controlled voltage sources can be expressed as follows:

$$
\begin{aligned} v_{ar} &= \omega[i_a \frac{d}{d\theta}L_{aa} + i_b \frac{d}{d\theta}L_{ab} + i_c \frac{d}{d\theta}L_{ac} + i_{kd} \frac{d}{d\theta}L_{akd} \\ &\quad + i_{kq} \frac{d}{d\theta}L_{akq} + i_{sd} \frac{d}{d\theta}L_{asd} + i_{sq} \frac{d}{d\theta}L_{asq}] \end{aligned} \tag{2}
$$

$$
\begin{aligned} v_{br} &= \omega[i_a \frac{d}{d\theta}L_{ba} + i_b \frac{d}{d\theta}L_{bb} + i_c \frac{d}{d\theta}L_{bc} + i_{kd} \frac{d}{d\theta}L_{bkd} \\ &\quad + i_{kq} \frac{d}{d\theta}L_{bkq} + i_{sd} \frac{d}{d\theta}L_{bsd} + i_{sq} \frac{d}{d\theta}L_{bsq}] \end{aligned} \tag{3}
$$

$$
\begin{aligned} v_{cr} &= \omega[i_a \frac{d}{d\theta}L_{ca} + i_b \frac{d}{d\theta}L_{cb} + i_c \frac{d}{d\theta}L_{cc} + i_{kd} \frac{d}{d\theta}L_{ckd} \\ &\quad + i_{kq} \frac{d}{d\theta}L_{ckq} + i_{sd} \frac{d}{d\theta}L_{csd} + i_{sq} \frac{d}{d\theta}L_{csq}] \end{aligned} \tag{4}
$$

$$
\begin{aligned} v_{kdr} &= \omega[i_a \frac{d}{d\theta}L_{kda} + i_b \frac{d}{d\theta}L_{kdb} + i_c \frac{d}{d\theta}L_{kdc} + i_{kd} \frac{d}{d\theta}L_{kdkd} \\ &\quad + i_{kq} \frac{d}{d\theta}L_{kdkq} + i_{sd} \frac{d}{d\theta}L_{kdsd} + i_{sq} \frac{d}{d\theta}L_{kdsq}] \end{aligned} \tag{5}
$$

$$
\begin{aligned} v_{kqr} &= \omega[i_a \frac{d}{d\theta}L_{kqa} + i_b \frac{d}{d\theta}L_{kqb} + i_c \frac{d}{d\theta}L_{kqc} + i_{kd} \frac{d}{d\theta}L_{kqkd} \\ &\quad + i_{kq} \frac{d}{d\theta}L_{kqkq} + i_{sd} \frac{d}{d\theta}L_{kqsd} + i_{sq} \frac{d}{d\theta}L_{kqsq}] \end{aligned} \tag{6}
$$

$$
\begin{aligned} v_{sdr} &= \omega[i_a \frac{d}{d\theta}L_{sda} + i_b \frac{d}{d\theta}L_{sdb} + i_c \frac{d}{d\theta}L_{sdc} + i_{kd} \frac{d}{d\theta}L_{sdkd} \\ &\quad + i_{kq} \frac{d}{d\theta}L_{sdkq} + i_{sd} \frac{d}{d\theta}L_{sdsd} + i_{sq} \frac{d}{d\theta}L_{sdsq}] \end{aligned} \tag{7}
$$

$$
\begin{aligned} v_{sqr} &= \omega[i_a \frac{d}{d\theta}L_{sqa} + i_b \frac{d}{d\theta}L_{sqb} + i_c \frac{d}{d\theta}L_{sqc} + i_{kd} \frac{d}{d\theta}L_{sqkd} \\ &\quad + i_{kq} \frac{d}{d\theta}L_{sqkq} + i_{sd} \frac{d}{d\theta}L_{sqsd} + i_{sq} \frac{d}{d\theta}L_{sqsq}] \end{aligned} \tag{8}
$$

Writing the loop equations for the equivalent circuit network of Figure (3) yields the differential equations given by equation (1). Accordingly, Figure (3) is an equivalent representation of the state model of the PM generator given in equation (1).

Meanwhile, in the case of a PM generator whose rotor damping consists of only the damper bar cage, to the exclusion of the shorted ring (collar), the equivalent circuit model reduces to that given in Figure (4). For further details reference [8] should be consulted.

It should be pointed out that the dynamics of these equivalent networks are identical to the dynamics of the PM generator, subject to proper initial conditions and external constraints. The external constraints are stemming from the rectifier bridge network and the dc load, which are discussed next.

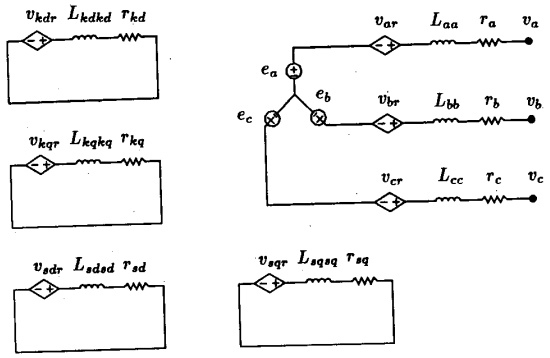

mutual inductances

1) $L_{ab}, L_{ac}, L_{akd}, L_{akq}, L_{asd}, L_{asq}$

2) $L_{ba}, L_{bc}, L_{bkd}, L_{bkq}, L_{bsd}, L_{bsq}$

3) $L_{ca}, L_{cb}, L_{ckd}, L_{ckq}, L_{csd}, L_{csq}$

4) $L_{kda}, L_{kdb}, L_{kdc}, L_{kdkq}, L_{kdsd}, L_{kdsq}$

5) $L_{kqa}, L_{kqb}, L_{kqc}, L_{kqkd}, L_{kqsd}, L_{kqsq}$

6) $L_{sda}, L_{sdb}, L_{sdc}, L_{sdkd}, L_{sdkq}, L_{sdsq}$

7) $L_{sqa}, L_{sqb}, L_{sqc}, L_{sqkd}, L_{sqkq}, L_{sqsd}$

Figure (3): PM Generator Equivalent Network Model Including Effects of Damper Cage and Damping Collar

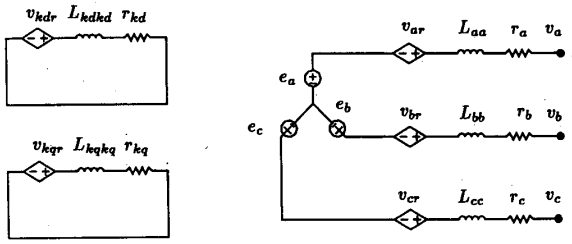

mutual inductances

1) $L_{ab}, L_{ac}, L_{akd}, L_{akq}$

2) $L_{ba}, L_{bc}, L_{bkd}, L_{bkq}$

3) $L_{ca}, L_{cb}, L_{ckd}, L_{ckq}$

4) $L_{kda}, L_{kdb}, L_{kdc}, L_{kdkq}$

5) $L_{kqa}, L_{kqb}, L_{kqc}, L_{kqkd}$

Figure (4): PM Generator Equivalent Network Model Including Effects of Damper Cage Only

SYSTEM NETWORK MODELING DESCRIPTION

The 75 kVA permanent magnet generator, whose cross-section is given in Figure (1), was modeled by the equivalent circuit shown in Figure (4) for the case when rotor damping is only due to the damper bar cage. In this network model, Figure (4), only the damper bars' equivalent damping circuits, kd and kq, exist. Now, the PM generator's equivalent circuit, Figure (4), can directly be merged with the rectifier-load network model. This results in the global equivalent network model of the PM generator-rectifier load system shown in Figure (5). Here, the nonlinear resistances, r_{D1} through r_{D6}, represent the diodes, D1 through D6, respectively. The dynamics of this network model are identical to the dynamics of the PM generator-rectifier load system, which include the effects of the damper bars only (no collar).

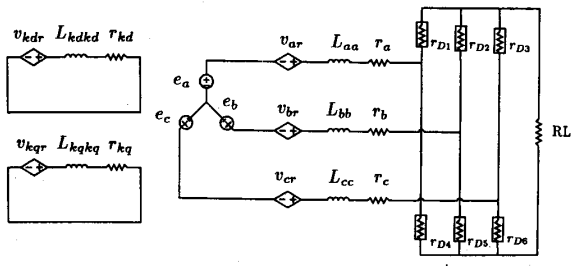

Figure (5): Machine-Rectifier Load Equivalent Network Model Including Effects of Damper Cage Only

Meanwhile, in order to study the impact of the addition of a rotor mounted damping ring (collar) on the PM generator-rectifier load system dynamic performance, the PM generator's equivalent circuit, Figure (3), which includes both the equivalent circuits of the damper bars and damping ring was used. Again, the PM generator's equivalent network, Figure (3), was merged with the rectifier-load network model. This resulted in the equivalent network model of the PM generator-rectifier load system, Figure (6). Again, the dynamics of this network model, Figure (6), are identical to the dynamics of the PM generator-rectifier load system including the effects of both the damper bar cage and the damping ring.

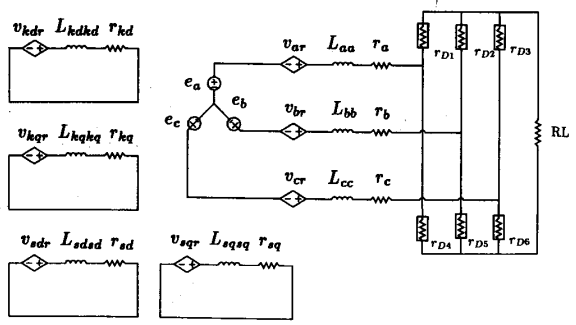

Figure (6): Machine-Rectifier Load Equivalent Network Including Effects of Damper Cage and Damping Collar

In the two network models of Figures (5) and (6), the self and mutual inductances L_{aa}, L_{ab}, $\cdots$, L_{sqsq}, were represented by Fourier series type expressions, which were determined from finite element magnetic field solutions in conjunction with the energy perturbation method, see references [7] and [8] for details. For the convenience of the reader and the sake of continuity, a set of these Fourier series inductance expressions, which was determined from field solutions at 1.0 p.u. load, is given in the Appendix. It should again be pointed out that these expressions enable one to include all the significant effects of space harmonics in the flux densities and flux linkages on the machine parameters and generator-rectifier system dynamics. This is a major advantage inherent in the natural abc frame of reference modeling approach given in this paper. In addition, the induced emfs, e_a, e_b, and e_c, were also represented by Fourier series type expressions which were determined using finite element field solutions, see the Appendix for these emf expressions [8].

Furthermore, when modeling the three phase full wave-rectifier diode-bridge, shown in Figures (5) and (6), attention was paid to the fact that the switching of the semiconductor devices (six diodes) between the "on", forward bias, and "off", reverse bias, states is continuously taking place throughout the normal operation of the generator-rectifier load system. Accordingly, these diodes were modeled as nonlinear bi-valued resistors , r_{D1} through r_{D6}, to simulate the "on" and "off" states.

Accordingly, by using generalized concepts of network graph theory in conjunction with hybrid matrix formulation of nonlinear networks [5,9], the state equations associated with the equivalent networks of the PM generator-rectifier load system, Figures (5) and (6), were automatically formulated and continuously updated in a computer-aided network solution program. In the following sections, the results of applying this numerical analysis approach to simulate and predict the sustained steady state dynamic performance of the PM generator-rectifier system at hand, as well as study the effects of electronic component failure in the associated rectifier bridge on this system's performance, are given.

DYNAMIC STEADY STATE ANALYSIS OF PERMANENT MAGNET GENERATOR-RECTIFIER LOAD SYSTEM

In order to perform a dynamic steady state analysis of the PM generator-rectifier load system, the global network model of Figure (5) was used. This network model includes only the effect of the damper bar cage (no collar). As mentioned above, the parameters of the permanent magnet generator were determined at 1.0 p.u. load condition, see the Appendix. A fourth order Runge-Kutta numerical solution method was used to solve for the state variables (inductor currents) in time. This resulted in all the voltage and current waveforms throughout the generator-rectifier load system. In addition, the approach was used to predict the currents in the various damper bars, as well as the power delivered to the dc load.

The computer simulated waveforms (CSWFs) of the phase (a) armature current, damper bar # 1 current, generator line to neutral (L-N) voltage, the current through and voltage across the diode, D1, as well as the dc load current, are given here in Figures (7) through (12), respectively. As can be seen in Figure (7), and as expected, the diode bridge commutation causes the slight dip in the middle of the phase current waveform. One of the major advantages of this modeling approach is the ability to reconstruct individual damper bar currents from the equivalent damping currents resulting from solution of the global networks, including effects of the various inherent space harmonics associated with the machine's winding and magnetic circuit configurations. For example, from this model the current in damper bar # 1 was determined, see Figure (8). Figure (8) demonstrates that the damper bars have a sustained (steady state) current of nonzero value, as expected from the physical nature of the resulting stator mmf. This is due to the continuous switching of the diodes in the rectifier load, which leads to a stator mmf that no longer rotates at the same speed of the rotor. Hence, there is a continuous relative motion between the armature mmf and the rotor mounted damper bars, which leads to perpetually induced currents in these bars. In order to determine the current in each of the fourteen damper bars embedded in the pole faces, Figure (1), the instantaneous values of i_{kd} and i_{kq}, at the end of each integration time step, were used. The current in each damper bar was determined as the result of superposition of the kd and kq contributions from i_{kd} and i_{kq}, respectively, as was detailed in an earlier work [8,10].

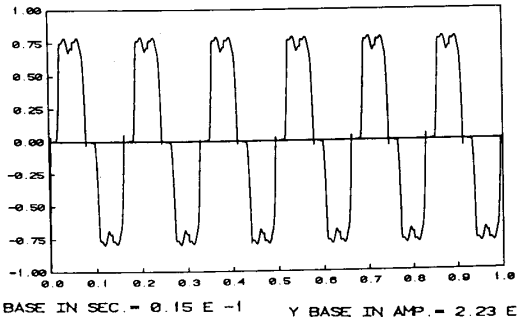

Figure (7): Machine Phase (a) Current - Damper Cage Only

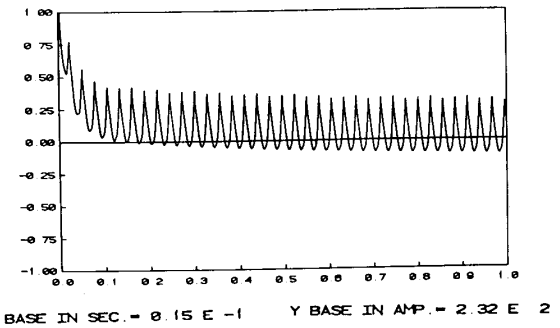

Figure (8): Damper Bar # 1 Current - Damper Cage Only

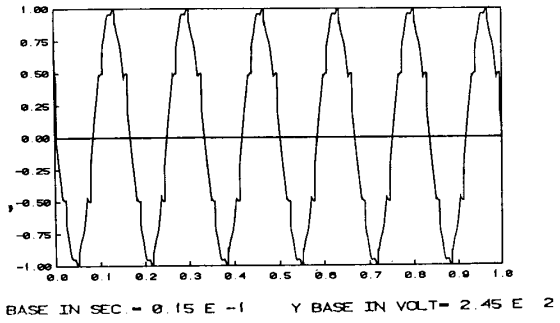

Figure (9): Machine L-N Voltage - Damper Cage Only

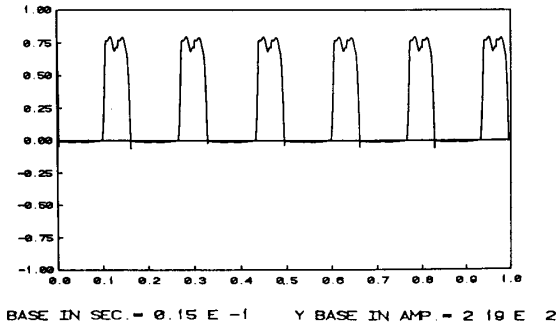

Figure (10): Rectifier Diode (D1) Current - Damper Cage Only

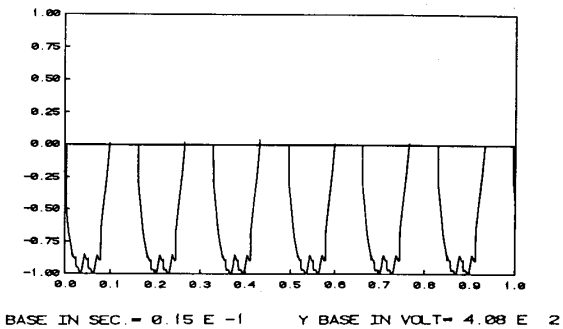

Figure (11): Rectifier Diode (D1) Voltage - Damper Cage Only

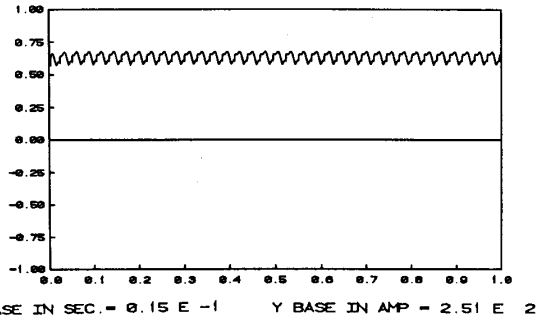

Figure (12): DC Load Current - Damper Cage Only

Also shown here are the CSWFs of the current through and voltage across diode, D1, Figures (10) and (11), respectively. As expected, the diode current is unidirectional. Furthermore, Figure (12) shows the CSWF of the dc load current. The profile of the dc load current was Fourier analyzed. As expected, the sixth harmonic is dominant. This is due to the switching of the six diodes that occurs during each ac cycle. Here also, an average value of 158.9 A was determined for the 1.0 p.u. load current. Furthermore, an average value of 60.74 kW was determined for the power delivered to the dc load.

In order to study the effects of including a rotor mounted damping ring (collar) in this PM generator on its performance, the network model of Figure (5) was used. In this network model the damping effects of both the damper bar cage and the damping ring are included. This resulted in the various current and voltage waveforms throughout the generator-load system. Here, the CSWFs of the phase (a) current, and the dc load current, are given in Figures (13) and (14), respectively. Here again, the dc load current data was Fourier analyzed. An average value of 160.6 A was obtained. Meanwhile, an average value of 62.14 kW was determined for the power delivered to the dc load. A discussion of these results is given in the following section.

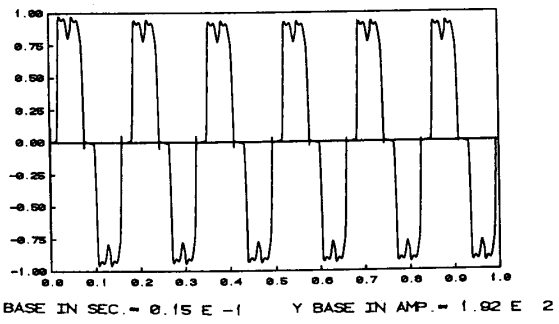

Figure (13): Machine Phase (a) Current - Damper Cage & Collar

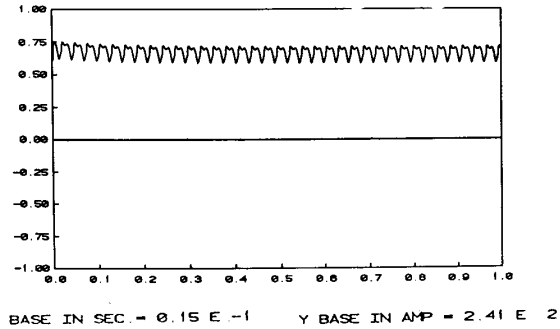

Figure (14): DC Load Current - Damper Cage & Collar

EFFECT OF DAMPING CIRCUITS ON GENERATOR LOAD SYSTEM POWER

In order to demonstrate the utility of this computer-aided method for design purposes, the model was used to evaluate the performance of three possible rotor design options for this 75 kVA permanent magnet generator. These rotor design options are as follows:

- Rotor Design Option #1 : Use for rotor damping a damper bar cage and a shorted damping ring (collar),
- Rotor Design Option #2 : Use for rotor damping a damper bar cage,
- Rotor Design Option #3 : Use no rotor damping windings (no bars, no collar).

As can be seen from the above discussion, the equivalent network model of Figure (6) must be used to predict the PM generator-rectifier load system performance when rotor design option #1 is implemented. Meanwhile, the equivalent network model of Figure (5) must be used to predict this generator system performance when rotor design option #2 is considered. Similarly, if one is to consider rotor design option #3, either equivalent circuit model of Figures (5) or (6) can be used provided the damping circuits are open circuited. These three options were studied here, and the results of the generator's peak phase current, the average dc load current, and average dc load power were obtained for this PM generator-rectifier load system for rotor design options #1 through #3. The results of these performance characteristics are given in Table (1).

Table 1: Effect of Damping Circuits on System Performance

PM Generator-Rectifier Load System Performance			
	Phase Current (Peak)	DC Current (Average)	Load Power (Average)
Cage + Collar	179.3 A	160.6 A	62.14 kW
Cage	176.3 A	158.9 A	60.74 kW
No Damping	175.8 A	157.3 A	59.52 kW

Examination of the predicted performance results of rotor design options # 1 through # 3, Table (1), reveals that the existence of two sets of damping windings on the rotor in option #1 as compared to the lack of rotor damping windings in option #3 leads to a rise in the output power capability of the system from 59.52 kW to 62.14 kW. This represents an increase of about 4.3% of generator output power with no change in armature winding design. This increase in generator output power and output current is expected with the addition of rotor damping circuits, since these circuits have the overall effect of lowering the machine impedance viewed from its terminals as part of the overall machine-load circuit. This is much the same phenomenon as the effects of secondary and tertiary windings in lowering the equivalent circuit impedance when viewed from the primary side of a three winding transformer.

USE OF THE MODEL IN STUDYING EFFECTS OF ELECTRONIC COMPONENTS FAILURE

Results of modeling electronic component failure in the associated rectifier bridge on the PM generator-rectifier load system performance, are given here. The type of fault simulated involves that of a diode failure leading to a short followed by an open circuit caused by fusing action. Here, the fault was assumed to take place after one third of the total simulation time has expired. This was done for computer-graphics purposes in order to compare the unfaulted and faulted behavior within one plot. In order to study the effect of a fault (shorted diode followed by an open circuit as a consequence of fuse action normally installed in such systems), the equivalent network of Figure (6) was used again. Here, the diode, D1, was short circuited for 10 integration time steps (62.5 μs), an approximation of the period it takes a fuse to produce an open circuit. This short circuit event of 62.5 μs was followed by open circuiting, D1, for the rest of the simulation time.

The simulation of the above mentioned fault and fault clearing sequence resulted in all voltage and current waveforms throughout the generator-load system. Here, the CSWFs for the phase (a) current, damper bar # 1 current, the current of diode, D1, the dc load current, and dc load power, are given in Figures (15) through (19), respectively. The effect of shorting the diode is apparent in all these waveforms. The magnitude of the diode current of Figure (17) increased sharply during the short, see the current spike of 397 A. Such excess of current leads to a fuse action which causes an open circuit in the rectifier bridge leg in which the fault occurred. As expected, after expiration of the short circuit event and the fuse action, the effect of the open diode in blocking portions of the phase (a) current is clearly demonstrated in Figure (15). Moreover, the unbalanced operating condition resulting from such fault caused, as expected, a decrease in the power delivered to the load. This effect is clearly demonstrated in the CSWF of the instantaneous load power given by Figure (19). Furthermore, the effect of this unbalanced operating condition is seen here by the higher current swings in damper bar #1, Figure (16). These current swings are attributed to the "negative sequence like" nature of the phase unbalance resulting from opening one of the three armature phases, which leads to a strengthened relative motion between the rotor's damper bars and the field created by the unbalanced armature currents. From the above, one can see that this modeling approach could be used effectively in a design process to arrive at appropriate dimensions for such damper bars. This is of great importance in such generator systems which feed electronically switched loads, because the damper bars should thermally withstand the magnitudes of the corresponding sustained induced currents. Again, these currents have sustained non zero values because of the continuous switching of the diodes in the rectifier bridge as was explained earlier in this paper.

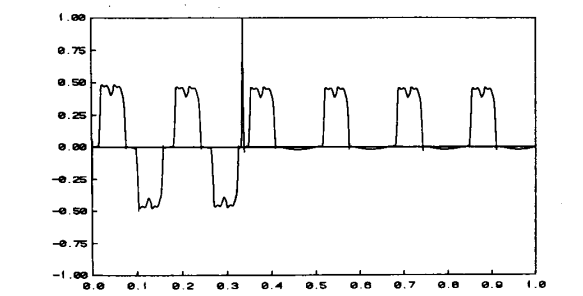

Figure (15): Machine Phase (a) Current (Shorted Diode Followed by Fuse Opening)

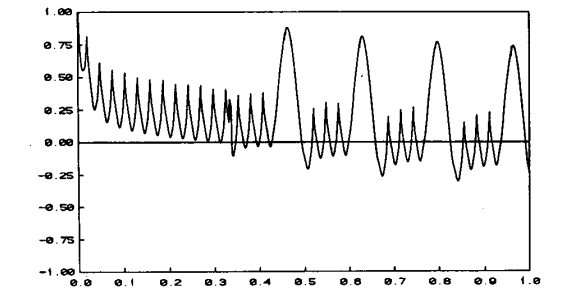

Figure (16): Damper Bar # 1 Current (Shorted Diode Followed by Fuse Opening)

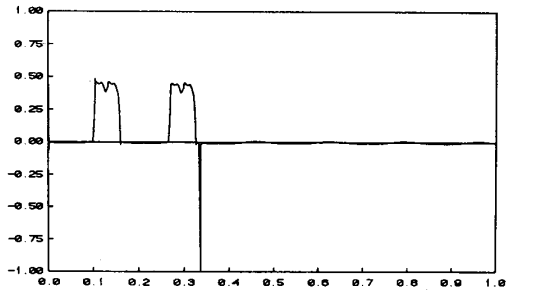

Figure (17): Rectifier Diode (D1) Current (Shorted Diode Followed by Fuse Opening)

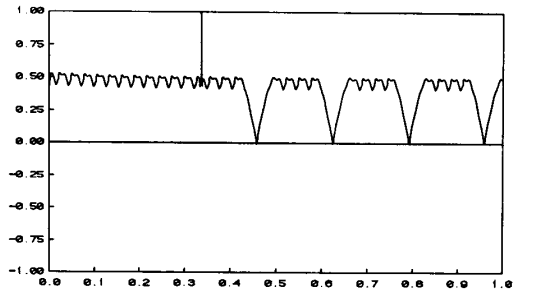

Figure (18): DC Load Current (Shorted Diode Followed by Fuse Opening)

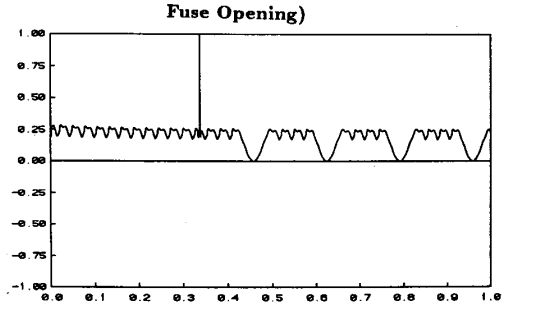

Figure (19): DC Load Instantaneous Power (Shorted Diode Followed by Fuse Opening)

CONCLUSIONS

In this paper, a computer-aided method was presented, by which one can analyze and predict the dynamic performance of a permanent magnet generator-electronically rectified load system with multiple damping circuits. This approach allows one to include the effects of the perpetually changing machine system network topologies caused by the continuous switching of the electronic devices. In this work, the natural abc frame of reference was used throughout. This facilitated the integration of the machinery and electronic components into a global model. Furthermore, this allowed the study of the effects of saliency and damping circuits on the system power as well as other performance characteristics. An advantage of using this approach is that it enables one to directly use readily available machine parameters obtained from finite element field solutions. Thus, the inherent nonlinearities and space harmonics in the flux linkages, inductances,

as well as induced emfs are fully accounted for in this modeling and analysis approach.

The approach was used also to study the effect of damping circuits on the output power of the PM generator load system through consideration of several rotor design options. It was found here that the inclusion of damping circuits in the design of such machines leads to higher output power. Here, an improvement of about 4.3 % in the power delivered to the load was achieved by adding the damper bar cage and the damping collar. The approach was used as well to study effects of electronic component failure on the machine system performance characteristics. As a result, computer simulated waveforms of currents and voltages were obtained for various machine system components. As expected, the continuous switching of the diodes in the rectifier bridge caused sustained non zero values of the currents induced in the damping circuits. As a result this modeling approach could be used effectively in a design process to arrive at appropriate dimensions of these damping conductors, to thermally withstand the magnitudes of the resulting induced currents.

Acknowledgment

These Authors wish to acknowledge the partial support by the Sundstrand Corporation, Rockford, Illinois, for the project on which this paper is partly based, under contract No. PO B-2L3493-247 with Clarkson University.

References

[1] Dvorscak, J.J., Lane, L.J., and Sinclair, C., " Shunt Thyristor Rectifiers for the GENERREX Excitation System", *IEEE Transactions on Power Apparatus and Systems,* Vol. PAS-96, No. 4, 1977, pp. 1219-1225.

[2] Chassande, J.P., Abdel-Razek, A.A., Poloujadoff, M., and Laumond, A., " Various Practical Results Concerning the Operation of Inverter Fed Self Controlled Synchronous Machines", *IEEE Transactions on Power Apparatus and Systems,* Vol. PAS-101, No. 12, 1982, pp. 4649-4655.

[3] Lipo, T.A. and Turnbull, F.B., "Analysis and Comparison of Two Types of Square Wave Inverter Drives", *IEEE Transactions on Industry Applications,* Vol. IA-11, No. 2, 1975, pp. 137-147.

[4] Demerdash, N.A. and Nehl, T.W., "Dynamic Modeling of Brushless DC Motors For Aerospace Actuation", *IEEE Transactions on Aerospace and Electronic Systems,* Vol. AES-16, No. 6, 1980, pp. 811-821.

[5] Nehl, T.W., Demerdash, N.A., Hijazi, T.M., and McHale, T.L., "Automatic Formulation of Models for Simulation of the Dynamic Performance of Electronically Commutated DC Machines", *IEEE Transactions on Power Apparatus and Systems,* Vol. PAS-104, No. 8, 1985, pp. 2214-2222.

[6] Arkadan, A.A., Hijazi, T.M., Demerdash, N.A., Vaidya, J.G., and Maddali, V.K., "Theoretical Development and Experimental Verification of a DC-AC Electronically Rectified Load-Generator System Model Compatible with common Network Analysis Software Packages", *IEEE Transactions on Energy Conversion,* Vol. EC-3, No. 1, 1988, pp. 123-131.

[7] Arkadan,A.A.,Demerdash,N.A., Vaidya,J.G., and Shah,M.J. "Impact of Load on Winding Inductances of Permanent Magnet Generators with Multiple Damping Circuits Using Energy Perturbation", Paper No. 88WM 001-0, presented at the IEEE-PES 1988 Winter Meeting, New York, and accepted for publication in the *IEEE-PES Transactions.*

[8] Arkadan A.A. "Computer-Aided Dynamic Performance Prediction of Permanent Magnet Generator Systems With Damping Circuits and Electronically Switched Loads", Ph.D. Dissertation, *Clarkson University,* January, 1988.

[9] Chua, L.O., and Lin, P., *Computer-Aided Analysis of Electrical Circuits: Algorithms and Computational Technique,* New Jersey: Prentice-Hall, Inc. 1975.

[10] Arkadan,A.A. and Demerdash,N.A.,"Modeling of Transients in Permanent Magnet Generators with Multiple Damping Circuits Using the Natural abc Frame of Reference", Paper No. 88WM 002-8, presented at the IEEE-PES 1988 Winter Meeting, New York, and accepted for publication in the *IEEE-PES Transactions.*

[11] Demerdash,N.A., Hijazi,T.M. and Arkadan A.A., "Computation of Winding Inductances of Permanent Magnet Brushless DC Motors with Damper Windings by Energy Perturbation", Paper No. 88WM 008-5, presented at the IEEE-PES 1988 Winter Meeting, New York, and accepted for publication in the *IEEE-PES Transactions.*

[12] Hijazi,T.M. and Demerdash,N.A., "Computer-Aided Modeling and Experimental Verification of the Performance of Power Conditioner Operated Permanent Magnet Brushless DC Motors Including Rotor Damping Effects", Paper No. 88WM 018-4, presented at the IEEE-PES 1988 Winter Meeting, New York, and accepted for publication in the *IEEE-PES Transactions.*

[13] Hijazi,T.M. and Demerdash,N.A., "Impact of the Addition of a Rotor-Mounted Damper Bar Cage on the Performance of Samarium-Cobalt Permanent Magnet Brushless DC Motor Systems," Paper No. 88WM 019-2, presented at the IEEE-PES 1988 Winter Meeting, New York, and accepted for publication in the *IEEE-PES Transactions.*

Appendix

Equations (1) through (16) of this Appendix, give the Fourier type expressions of the incremental inductances of the 75 kVA PM generator at 1.0 p.u. load in units of μH.

$$L_{aa}(\theta) = 30.454 - 0.794sin(2\theta) - 1.564cos(2\theta) + 0.091sin(6\theta) - 0.035cos(6\theta) \quad (1)$$

$$L_{ab}(\theta) = -14.904 - 0.889sin(2\theta) + 1.471cos(2\theta) - 0.046sin(6\theta) + 0.016cos(6\theta) \quad (2)$$

$$L_{kdkd}(\theta) = 0.580 \quad (3)$$

$$L_{akd}(\theta) = 2.41cos(\theta) \quad (4)$$

$$L_{kqkq}(\theta) = 5.308 \quad (5)$$

$$L_{akq}(\theta) = -10.796sin(\theta) \quad (6)$$

$$L_{sdsd}(\theta) = 0.387 \quad (7)$$

$$L_{asd}(\theta) = -0.77sin(\theta) + 2.406cos(\theta) \quad (8)$$

$$L_{sqsq}(\theta) = 4.995 \quad (9)$$

$$L_{asq}(\theta) = -4.04sin(\theta) + 0.265cos(\theta) \quad (10)$$

$$L_{kdkq}(\theta) = 0.019 \quad (11)$$

$$L_{kdsd}(\theta) = 0.208 \quad (12)$$

$$L_{kdsq}(\theta) = 0.019 \quad (13)$$

$$L_{kqsd}(\theta) = 0.019 \quad (14)$$

$$L_{kqsq}(\theta) = 1.430 \quad (15)$$

$$L_{sdsq}(\theta) = 0.021 \quad (16)$$

Equations (17) through (19) give the emf expressions in units of Volts:

$$e_a(\theta) = -241.17sin(\theta) + 2.45sin(7\theta) - 4.00sin(11\theta) + 2.03sin(13\theta) \quad (17)$$

$$e_b(\theta) = -241.17sin(\theta - 2\pi/3) + 2.45sin(7\theta - 2\pi/3) - 4.00sin(11\theta - 4\pi/3) + 2.03sin(13\theta - 2\pi/3) \quad (18)$$

$$e_c(\theta) = -241.17sin(\theta - 4\pi/3) + 2.45sin(7\theta - 4\pi/3) - 4.00sin(11\theta - 2\pi/3) + 2.03sin(13\theta - 4\pi/3) \quad (19)$$

For details on computer-aided determination of these expressions, reference [8] should be consulted.

A. A. ARKADAN was born in Sidon-Lebanon on June 1, 1956. He received his B.S. degree in Electrical Engineering (Magna Cum Lauda) from the University of Mississippi in 1980. In August, 1981 he received his M.S. degree in Electrical Engineering from Virginia Polytechnic Institute and State University. In January, 1988 he received his Ph.D. from Clarkson University. During the period 1981-1984 he worked in industry as a design and quality control engineer in Saudi Arabia. During the Summers of 1985 and 1986 he worked in Aviation Operations at Sundstrand Corporation, Rockford, Illinois, where he developed software packages for modeling and analysis of generator-rectified load systems and motor-inverter drive systems for aerospace applications.

Dr. Arkadan is currently an Assistant Professor of Electrical Engineering at Marquette University in Milwaukee, Wisconsin. His interests include: design, analysis, and development of electronically operated machine systems and drives, computer-aided solution of electromagnetic field problems in electrical devices, and time domain analysis of distributed and lumped parameter electrical and electronic systems.

Dr. Arkadan is a member of IEEE, ASEE, Phi Kappa Phi, Pi Mu Epsilon, Eta Kappa Nu, and Tau Beta Pi.

TOUFIC M. HIJAZI was born in 1957 in Sidon, Lebanon. He received the B.S.E.E. degree (Magna Cum Lauda) from the University of Mississippi in 1980, the M.Sc. degree in Electrical Engineering from Virginia Polytechnic Institute and State University in 1981, and the Ph.D. degree from Clarkson University in 1988.

From 1981 to 1984 he was with Saudi Oger Ltd. Company in Riyadh, Saudi Arabia. During the Summer of 1985 he was with the Aviation Operations of Sundstrand Corporation, Rockford, Illinois, working on Synchronous Generators with Rectified DC Loads for Aerospace Applications. As of September 1, 1988, he is a Senior Project Engineer with the Advanced Engineering Staff of General Motors Corporation, Warren, Michigan.

Dr. Hijazi is a member of IEEE. He is also a member of Phi Kappa Phi, Tau Beta Pi, Eta Kappa Nu, and Pi Mu Epsilon. His current interests and research activities include computer-aided modeling of the dynamic performance of drive systems, power electronics, and numerical computation of electromagnetic fields in electrical devices.

NABEEL A. DEMERDASH (M65, SM74) was born on April 26, 1943 in Cairo, Egypt. He earned his B.Sc.E.E. (Distinction with First Class Honors) from Cairo University in 1964, and imigrated to the U.S. in 1966 where he earned his M.S.E.E. and Ph.D. degrees from the University of Pittsburgh, Pittsburgh, PA in 1967 and 1971, respectively. From 1966 to 1968 he was a teaching assistant in the Department of Electrical Engineering, University of Pittsburgh. From 1968 to 1972 he was a development engineer with the Westinghouse Electric Corporation, Large Rotating Apparatus Development Engineering Department, East Pittsburgh, PA. From 1972 to 1983 he held the positions of assistant professor, associate professor, and professor, respectively, in the Department of Electrical Engineering at Virginia Polytechnic Institute and State University, Blacksburg, VA. Since 1983 he has held the position of professor in the Department of Electrical and Computer Engineering, Clarkson University, Potsdam, NY. Professor Demerdash has consulted and performed research for many corporations and government agencies such as the Ford Motor Company, Sundstrand Corporatioon, Honeywell Avionics, the Middle Atlantic Power Research Committee, NASA, NASA-DOE, the U.S. Air Force, and Westinghouse Electric Corporation.

Dr. Demerdash is active in the Rotating Machinery Committee of PES-IEEE, and its various subcommittees, where he is presently the Chairman of its DC and Permanent Magnet Machinery Subcommittee. He is also a member of the Continuing Education Subcommittee of PEEC, PES-IEEE. He is the author and/or coauthor of more than 120 publications of which more than 50 are IEEE Transactions and Other Journal Papers on numerical analysis of electromagnetic fields, computer-aided design and analysis of electronically operated high speed electric machinery systems and drives, as well as computer-aided lumped parameter-distributed parameter modeling and design of electromechanical systems. Professor Demerdash's current interests and research activities include power electronics applications to electric machinery and drive systems, space station solar dynamic power generation and system dynamics, electromechanical propulsion and actuation, numerical analysis of electromagentic fields in electrical and electronic devices, as well as computer-aided modeling of machine-power system harmonic effects on their dynamics.